0026-895X/04/6601-169–177$20.00
MOLECULAR PHARMACOLOGY
Vol. 66, No. 1
3162/1162237
Mol Pharmacol 66:169–177, 2004
Printed in U.S.A.

A Single Point Mutation Confers Properties of the Muscle-Type Nicotinic Acetylcholine Receptor to Homomeric α7 Receptors

Andon N. Placzek, Francesca Grassi, Thaddeus Papke, Edwin M. Meyer, and Roger L. Papke

Department of Pharmacology and Therapeutics, J. Hillis Miller Health Science Center, University of Florida, Gainesville, Florida (A.N.P., T.P., E.M.M., R.L.P.); and Istituto Pasteur-Fondazione Cenci Bolognetti and Dipartmento di Fisiologia Umana e Farmacologia, Universita' di Roma "La Sapienza", Roma, Italy (F.G.)

Received December 16, 2003; accepted April 21, 2004

This article is available online at http://molpharm.aspetjournals.org

ABSTRACT

Although the muscle-type and homomeric α7-type nicotinic acetylcholine receptors (nAChRs) share many structural features and bind α-bungarotoxin with high affinity, several important functional and pharmacological properties distinguish these two major nAChR subtypes. We have shown previously that amino acid sequence in the second transmembrane (TM) domain of the β subunit is critical for pharmacological distinction between muscle type and heteromeric neuronal (e.g., ganglionic) nAChRs. We tested the hypothesis that homologous substitution of amino acid sequence from the muscle β1 subunit into the α7 subunit would confer specific properties of muscle-type receptors to mutant α7 nAChRs. In this study, we show that a single amino acid substitution at the α7 TM2 6′ position makes both biophysical and pharmacological properties of the mutant receptors resemble those of wild-type muscle nAChR. This mutation produces significant changes in acetylcholine potency and response kinetics, eliminating the characteristic fast desensitization of α7 and dramatically reducing divalent ion permeability relative to wild-type α7. The TM2 T6′F mutation also produces a profound increase in activation by succinylcholine compared with either wild-type α7 or neuronal β-subunit–containing receptors and the loss of potentiation by 5-hydroxyindole. Thus, the α7 TM2 T6′F mutant displays several features that are similar to the muscle nAChR, some of which are not typically thought to be regulated by the pore-lining domain of the receptor.

Nicotinic acetylcholine receptors have long been recognized as the primary postsynaptic effector in vertebrate neuromuscular transmission, as well as having a clearly established role in ganglionic neurotransmission. In recent years, nicotinic receptors have also been identified as important functional molecules in central neurons (reviewed in McGehee and Role, 1995; Dani, 2001). Based on differences in function, pharmacology, and tissue distribution, it is possible to categorize the larger family of nAChRs broadly into three major subfamilies. These are the muscle-type receptors, the neuronal β-subunit–containing receptors that bind agonist with relatively high affinity in the desensitized state, and the homomeric α-subunit receptors, typified by α7.

Concomitant with the evolution of these diverse forms of the nAChR and the functional radiation of these receptor subtypes into various tissues, where each subtype performs highly specialized functions, a large amount of sequence divergence has emerged. There is less than 40% amino acid sequence identity between the α-subunit of muscle type receptors (α1) and the α7-type receptor found in the brain. It has generally been assumed that the functional differences that exist among these receptor subtypes are emergent properties of the collective sequence differences. Nonetheless, it is well appreciated that specific residues, conserved across multiple subtypes, can be key to features common to all those subtypes. Several such foci of important conserved sequence are in the pore-forming second transmembrane domain; in this domain the sequence identity between α1 and α7 is increased to 60%.

Both muscle-type nAChR and homomeric α7 receptors are widely expressed in mammals and bind the snake toxin, α-Btx. Despite these similarities, there are numerous important functional and pharmacological differences between the muscle and α7-type receptors. For example, α7 receptors have high divalent ion permeability, show inwardly rectifying current-voltage relationships, and have unique agonist concentration-dependent macroscopic

This work was supported by National Institutes of Health grants NS043822-01A, GM57481-01A2, and P01-AG10485.

ABBREVIATIONS: nAChR, nicotinic acetylcholine receptor; α-Btx, α-bungarotoxin; TM2, transmembrane domain; ACh, acetylcholine; MS222, 3-aminobenzoic acid ethyl ester; BAPTA, 1,2-bis(2-aminophenoxy)ethane-*N*,*N*,*N*′,*N*′-tetraacetic acid; MLA, methyllycaconitine; KRH, Krebs-Ringer-HEPES; 5HI, 5-hydroxyindole; GHK, Goldman-Hodgkin-Katz; SuCh, succinylcholine.

response kinetics (Decker and Dani, 1990; Sands et al., 1993; Seguela et al., 1993; Vernino et al., 1994).

Previous work in our laboratory has indicated that amino acid residues in the TM2 domain of the β subunit of heteromeric nAChRs are important regulators of nAChR pharmacology. In particular, substitution of the TM2 6′ [according to the numbering scheme proposed by Miller (1989); see Fig. 1] phenylalanine of the muscle β1 subunit for the neuronal β4 subunit serine residue increased sensitivity to nicotine. This study also showed that substitution of β1 subunit amino acid sequence at the TM2 6′ and 10′ positions of the neuronal β4 subunit reduced inhibition by the ganglionic blocker mecamylamine (Webster et al., 1999). Based on these previous observations, we hypothesized that substitution of β1 subunit amino acid sequence in the α7 TM2 would change specific properties of the mutant homomeric receptors so that they would more closely resemble muscle-type nAChRs. Using site-directed mutagenesis and heterologous expression of mutant receptors in *Xenopus laevis* oocytes, we tested the effect of a T6′F mutation in α7 on ACh potency, ACh response kinetics, barium permeability, the sensitivity to the muscle receptor selective agonist succinylcholine, and the α7 potentiating factor 5-hydroxyindole.

Materials and Methods

cDNA Clones. These experiments used the rat neuronal nAChR and the mouse muscle cDNA clones, which were obtained from Dr. Jim Boulter (UCLA). The sequences of the TM2 domains of the relevant subunits are shown in Fig. 1. Adopting the terminology proposed by Miller (1989), the 20 residues in the putative second transmembrane sequence are identified as 1′ through 20′.

Site-Directed Mutagenesis. Site-directed mutagenesis was performed using QuikChange kits (Stratagene, LaJolla, CA). In brief, two complimentary oligonucleotides were synthesized that contained the desired mutation flanked by 10 to 15 bases of unmodified nucleotide sequence. Using a thermal cycler, *Pfu* DNA polymerase extended the sequence around the whole vector, generating a plasmid with staggered nicks. Each cycle built only off the parent strands; therefore there was no amplification of misincorporations. After 12 to 16 cycles, the product was treated with DpnI, which digested the methylated parent DNA into numerous small pieces. The product was then transformed into *Escherichia coli* cells, which repaired the nicks.

Preparation of RNA. After linearization and purification of cloned cDNAs, RNA transcripts were prepared in vitro using the appropriate mMessage mMachine kit from Ambion Inc. (Austin, TX).

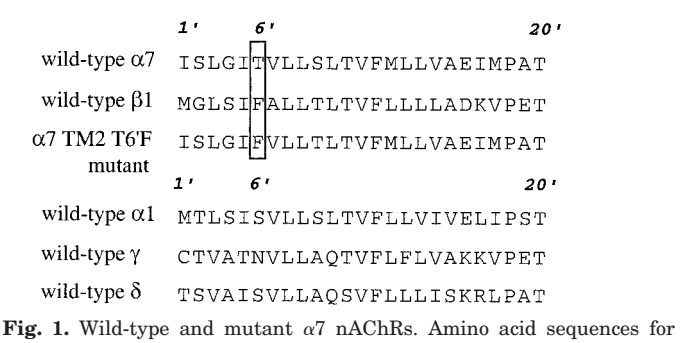

Fig. 1. Wild-type and mutant α7 nAChRs. Amino acid sequences for wild-type and mutant α7 nAChR TM2 domains. The numbering of specific residues of the second membrane-spanning region is according to that proposed by Miller (1989). The corresponding sequences for wild-type muscle β1, γ, and δ subunits are also given as a reference. The substituted residue is highlighted at the 6′ position.

Expression in *X. laevis* Oocytes. Mature (>9 cm) female *X. laevis* African toads (Nasco, Ft. Atkinson, WI) were used as a source of oocytes. Before surgery, frogs were anesthetized by placing the animal in a 1.5 g/liter solution of MS222. Oocytes were removed from an incision made in the abdomen.

To remove the follicular cell layer, harvested oocytes were treated with collagenase from Worthington Biochemical Corporation (Freehold, NJ) for 2 h at room temperature in calcium-free Barth's solution (88 mM NaCl, 10 mM HEPES, pH 7.6, 0.33 mM $MgSO_4$, and 0.1 mg/ml gentamicin sulfate). Thereafter, stage 5 oocytes were isolated, and each was injected with 50 nl of a mixture of the appropriate subunit cRNAs after harvest. Recordings were made 3 to 21 days after injection depending on the cRNAs being tested. To increase the magnitude of the functional responses from oocytes injected with the T6′F mutant, approximately 5 times (30 ng) the amount of mutant mRNA was injected compared with wild-type α7 (approximately 6–7 ng). Because all data were normalized using each cell as its own control, absolute differences in response magnitude did not affect comparisons between receptor subtypes.

Voltage-Clamp Recording of Whole-Oocyte Responses. Data were obtained by means of two-electrode voltage-clamp recording. Recordings were made at room temperature (21–24°C) in frog Ringer's solution (115 mM NaCl, 10 mM HEPES, 2.5 mM KCl, and 1.8 mM $CaCl_2$, pH 7.3) with 1 μM atropine to inhibit muscarinic acetylcholine receptor responses. This extracellular solution was used for all experiments unless otherwise noted. Voltage electrodes were filled with 3 M KCl, and current electrodes were filled with 250 mM CsCl, 250 mM CsF, and 100 mM EGTA, pH 7.3.

Bath solution and drug applications were applied through a linear perfusion system to oocytes placed in a Lucite chamber with a total volume of 0.5 ml. Drug delivery involved preloading a 1.8-ml section of tubing at the terminus of the perfusion system, while a Mariotte flask filled with Ringer's solution was used to maintain constant perfusion. Applications of drug solutions were then synchronized with acquisition. Current responses were recorded using a PC interfaced to either a Warner OC-725C (Warner Instruments, Hamden, CT) or a GeneClamp 500 amplifier via a Digidata 1200 digitizer (Axon Instruments, Union City, CA). In addition, some oocyte recordings were made using a beta version of the OpusXpress 6000A (Axon Instruments). OpusXpress is an integrated system that provides automated impalement and voltage clamp, which in our case permitted the study of four oocytes in parallel. Cells were automatically perfused with bath solution, and agonist solutions were delivered from a 96-well compound plate. In experiments using the OpusXpress system, the voltage and current electrodes were filled with 3 M KCl. In all experiments, bath flow rates were set at 2 ml/min.

Experimental Protocols and Analysis of Data from *X. laevis* Oocytes. Current responses to drug application were studied under two-electrode voltage clamp at a holding potential of −50 mV unless otherwise noted (−60 mV for the OpusXpress system). Holding currents immediately before agonist application were subtracted from measurements of the peak response to agonist. All drug applications were separated by a wash period of 5 min unless otherwise noted. At the start of recording, all oocytes received two initial control applications of ACh. Subsequent drug applications were normalized to the second ACh application to control for the level of channel expression in each oocyte. Means and S.E.M. were calculated from the normalized responses of at least four oocytes for each experimental concentration. For concentration-response relations, data were plotted using Kaleidagraph 3.0.2 (Abelbeck/Synergy Software, Reading, PA), and curves were generated using the Hill equation: Response = $(I_{max}[agonist]^{nH}) / ([agonist]^{nH} + (EC_{50})^{nH})$, where I_{max} denotes the maximal response for a particular agonist/subunit combination, and n_H represents the Hill coefficient. I_{max}, n_H, and the EC_{50} were all unconstrained for the fitting procedures.

For experiments measuring barium permeability, oocytes were perfused with barium Ringers (low barium: 90.7 mM NaCl, 2.5 mM

KCl, 10 mM HEPES, pH 7.3, 1.8 mM $BaCl_2$, and 48.6 mM sucrose; high barium: 90.7 mM NaCl, 2.5 mM KCl, 10 mM HEPES, pH 7.3, and 18 mM $BaCl_2$). Shifts in reversal potential were measured by changing the holding potential from −40 to +30 mV by 10-mV increments. Calculations of barium/sodium permeability ratios using the extended GHK equation were performed using the Clampfit analysis portion of the pClamp software suite (Axon Instruments). Barium was used instead of calcium to minimize the contribution of endogenous calcium-activated chloride channels (Sands et al., 1993).

Calculations of peak amplitudes and net charge were made using pClamp either during acquisition or during subsequent Clampfit analysis. Note that measurement of net charge has been shown to be a more accurate indicator of fast α7 responses than measurement of peak response. An appropriate method using analysis of the area under the curve of agonist-evoked currents in oocytes has been published previously (Papke and Papke, 2002). Baseline was defined for Clampfit statistics based on 20 s before drug application, the analysis region for peak and net charge analysis went from 5 s before the initiation of drug application and extended at least 135 s after. Area analysis data are provided for all receptor subtypes examined in this article for comparison to wild-type α7.

Transfection and Whole-Cell Voltage Clamp Recording from GH4C1 Cells. GH4C1 cells were cultured in F10 medium (Invitrogen, Carlsbad, CA) at 37°C, 5% CO_2. Cells were transiently transfected using Fugene (Roche, Indianapolis, IN), according to the manufacturer instructions. One microgram of wild-type or T6′F mutant α7 cDNA (pTR-UF22; University of Florida, Gainesville, FL) was added to each 35-mm Petri dish, together with 0.5 or 1 μg of the cDNA encoding the red fluorescent DsRed protein (BD Biosciences Clontech, Palo Alto, CA). Cells were used 48 to 72 h after transfection. Typical transfection efficiency was 10 to 25% using this method.

Whole-cell currents were recorded using an Axopatch 200B amplifier (Axon Instruments) at room temperature. Cells were bathed in a solution containing 140 mM NaCl, 2.8 mM KCl, 2 mM $CaCl_2$, 2 mM $MgCl_2$, 10 mM glucose, and 10 mM HEPES/NaOH, pH 7.3. Patch electrodes (tip resistances, 3–5 MΩ) were filled with 140 mM CsCl, 5 mM BAPTA, 2 mM Mg-ATP, and 10 mM HEPES/CsOH, pH 7.3. Cells were continuously superfused by a gravity-driven fast-exchanging perfusion system (RSC 200; BioLogic, Claix, France), with independent tubes for each solution placed ~100 μm from the cells. Currents were recorded at 2 KHz using pClamp 8 (Axon Instruments), at a membrane holding potential of −70 mV, unless otherwise indicated. Analysis was conducted using pClamp 8.

Radioligand Binding Studies. GH4C1 cells were harvested from 60-mm culture dishes using a sterile cell scraper and assayed for nicotine-displaceable, high-affinity [^{3}H]methyllycaconitine (MLA) binding using a modification of the procedure of Davies et al. (1999). Cells were suspended in 20 volumes of ice-cold Krebs-Ringer-HEPES buffer (KRH; 118 mM NaCl, 5 mM KCl, 10 mM glucose, 1 mM $MgCl_2$, 2.5 mM $CaCl_2$, and 20 mM HEPES, pH 7.5). After two 1-ml washes with KRH at 20,000*g*, the membranes were incubated in 0.5 ml of KRH with 1, 3, 10, or 20 nM [^{3}H]MLA (Tocris, Ellisville, MO) for 60 min at 4°C with or without 5 mM nicotine. Tissues were washed three times with 5 ml of ice-cold KRH by filtration through Whatman GF/C filters that had been preincubated for 2 h in bovine lacto-transfer optimizer (KRH with 0.5% dry milk and 0.002% sodium azide). They were then assayed for radioactivity using liquid scintillation counting. Inhibition curves generated under two-electrode voltage-clamp with oocytes expressing either wild-type α 55 or the TM2 T6′F mutant showed a less than 3-fold difference in MLA potency between the two (data not shown).

^{125}I-α-Bungarotoxin binding in intact oocytes was performed similar to the method described by Chang and Weiss (1999) and later by Fenster et al. (1999). In brief, whole *X. laevis* oocytes that were either uninjected or had been injected with mRNAs encoding either wild-type α7 or the TM2 T6′F mutant were placed in a single well of a 96-well plate containing either 20 nM ^{125}I-α-Btx alone, or 20 nM ^{125}I-α-Btx with 5 mM nicotine. After four 4-s washes in 2.5 ml of KRH, total radioactivity was measured using an automated γ particle counter (counts per minute). Nicotine displaceable binding was calculated for at least four cells in each condition.

Results

The α7 TM2 T6′F Mutant Is Functionally Expressed by Oocytes. Two different cell systems, *X. laevis* oocytes and the GH4C1 cell line, were evaluated for functional expression of wild-type or mutant nAChRs. GH4C1 cells produced detectable currents under whole-cell voltage-clamp when transfected with a wild-type α7 construct, but no measurable currents were present in cells transfected with the TM2 T6′F mutant (data not shown). Injection of mRNAs encoding either wild-type or mutant α7 subunits in *X. laevis* oocytes produced functional receptors that permitted us to study the receptors under two-electrode voltage clamp. Raw data traces from oocytes expressing the TM2 T6′F point mutation or wild-type α7 are shown in Fig. 2. Differences between mutant and wild-type α7 receptors were seen both in the macroscopic response kinetics (Fig. 2, inset) and in the absolute amplitude of the response to ACh. There was consistently a relatively small peak for the T6′F response compared with the wild-type α7 response. Quantification of differences in absolute amplitude is complicated by variations in the degree of receptor expression from cell to cell. However, variations in current amplitude similar to those shown in Fig. 2 were consistently observed, even after oocytes expressing the mutant receptor were kept for several weeks to allow receptor expression to accumulate. Because of this difference in functional expression, oocytes expressing mutant receptors were typically used 11 to 21 days after injection, whereas oocytes expressing wild-type receptors were used 5 to 14 days after injection. The average amplitude of control responses (3

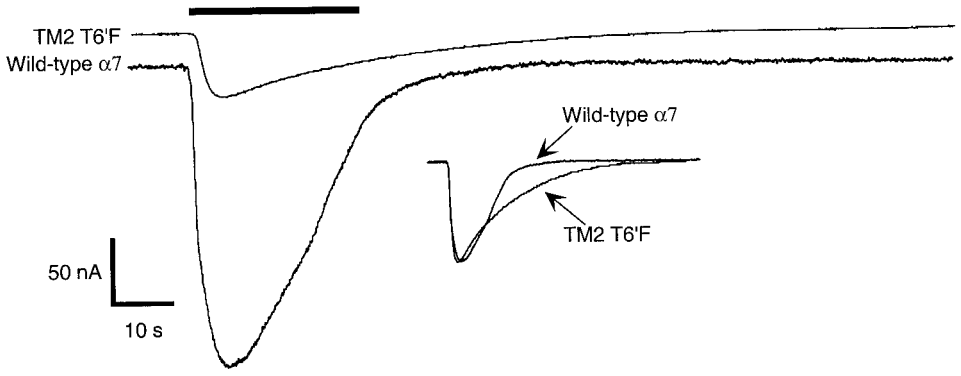

Fig. 2. Electrophysiological responses from wild-type and mutant α7 nAChRs. ACh-evoked current responses for wild-type α7 and the TM2 T6′F mutant nAChR expressed in oocytes. The agonist application bar at the top indicates the timing and duration of agonist application for each receptor (wild-type, 30 μM ACh; T6′F, 3 μM ACh). The inset shows the same traces scaled to one another for the purpose of comparison (wild-type, 100%; T6′F, 476%).

μM ACh) of mutant receptor responses recorded 11 to 21 days after injection was 64.5 ± 12 nA (n = 12), whereas the average amplitude of control responses (300 μM ACh) of wild-type receptor responses recorded 5 to 14 days after injection was 335.9 ± 60 nA (n = 12). These concentrations of ACh were chosen for controls because the normalized area under the curve of these responses was at the upper end of the concentration-response function, and they are therefore roughly saturating in terms of net charge. It is important to note that the 100-fold difference in control ACh concentrations is caused by the increase in ACh potency observed in the T6′F mutant (see Fig. 4).

To determine whether differences in current magnitude between wild-type α7 and the T6′F mutant were caused by a relatively low mutant receptor expression at the cell surface or by an effect of the mutation on single channel properties (i.e., the probability of channel opening or single-channel conductance), radioligand binding experiments were performed with both the transfected GH4C1 cells and intact oocytes. In the case of the transfected GH4C1 cells, [^{3}H]MLA binding experiments conducted 48 h after transfection indicated an approximate B_{max} of 600 fmol/mg of total protein in cells transfected with wild-type α7, but no significant nicotine-displaceable binding was observed in cells transfected with the T6′F mutant relative to nontransfected cells (data not shown). However, single oocyte ^{125}I-α-Btx binding studies indicated significant specific binding in oocytes injected with either the wild-type α7 or the T6′F mutant (Table 1). These same experiments also showed no significant difference in ^{125}I-α-Btx binding between intact oocytes expressing either wild-type α7 or the T6′F mutant. Thus, it is likely that poor (or possibly slow) expression of the TM2 T6′F mutant receptors prevented their study in transfected GH4C1 cells but that alterations in receptor number alone were insufficient to explain the differences in current magnitude between wild-type and mutant receptors expressed in *X. laevis* oocytes.

TABLE 1

Intact oocyte ^{125}I-α-Btx binding

Data represent the mean (± S.E.M.) counts per minute per cell for the indicated treatments.

	cpm/cell
Rat α7 wild-type	
20 nM α-Btx alone	764.32 ± 529.4 (n = 4) *
20 nM α-Btx + 5 mM nicotine	72.15 ± 60.5 (n = 4)
Rat α7 T6′F mutant	
20 nM α-Btx alone	1074.98 ± 418.8 (n = 4) *
20 nM α-Btx + 5 mM nicotine	261.55 ± 137.5 (n = 3)

* $P \leq 0.05$ by Student's t test compared with the same receptor subtype in the presence of 20 nM α-Btx with 5 mM nicotine.

TABLE 2

Curve-fit values for wild-type and T6′F mutant α7 responses to ACh

Data represent curve values generated by the Hill equation (see *Materials and Methods*) for macroscopic responses from oocytes expressing either indicated receptor.

	Normalized I_{max}	Hill Coefficient	EC_{50}
Rat α7 wild-type			
ACh peak [a]			
ACh net charge	1.05 ± 0.02	1.5 ± 0.1	16.5 ± 1.0 μM
Rat α7 T6′F mutant			
ACh peak	0.89 ± 0.04	1.5 ± 0.4	1.7 ± 0.4 μM
ACh net charge	0.96 ± 0.04	2.4 ± 1.1	1.1 ± 0.2 μM

[a] The use of peak responses has been shown to provide inaccurate estimates of these parameters (Papke and Papke, 2002) and curve-fitting was thus restricted to net charge analysis for wild-type α7.

The α7 TM2 T6′F Mutation Dramatically Slows the Apparent Kinetics of ACh-Evoked Macroscopic Currents. The wild-type α7 receptor response has a characteristically rapid time course when high concentrations of ACh are applied; the decay phase occurs well before the bath solution exchange is complete (Papke and Thinschmidt, 1998; Papke and Papke, 2002). As shown in Fig. 3, the α7 TM2 T6′F mutation produced a dramatic change in the apparent kinetics of ACh responses. Figure 3C shows the relative lack of effect of increasing concentrations of ACh on duration of the macroscopic responses of the T6′F mutants, distinct from both wild-type α7 (Fig. 3A) and the muscle-type nAChR (Fig. 3B). This would be consistent with a change in receptor desensitization. Quantitative analysis is shown in Fig. 3, D and E. This shows the detailed effects of this point mutation on both the time required to reach the peak response and the return to baseline. Here it is evident that both the rise times and the decay times of the T6′F mutant showed little sensitivity to changes in ACh concentration, which is different from the characteristically concentration-dependent kinetics of the wild-type α7 response to ACh. The rise times of wild-type α7 responses differed from those of both the T6′F mutant and muscle nicotinic receptors at ACh concentrations $\leq$30 μM. The rise times of muscle receptors were also relatively insensitive to changing ACh concentrations compared with wild-type α7. In the case of the decay times, muscle receptors display concentration dependence, but it is the opposite of that seen with wild-type α7, with a general slowing of the decay of the muscle-type macroscopic response with increasing agonist concentration. Thus, we see that the macroscopic responses of the mutant and wild-type α7 receptors and the muscle-type receptors are each uniquely affected by the process of agonist wash-in and wash-out, presumably because of differences in their intrinsic desensitization rates and the influence of agonist binding on those rates (as proposed for wild-type α7). We have measured the kinetics of solution exchange in our oocyte bath perfusion system (Papke and Thinschmidt, 1998; Papke and Papke, 2002), allowing us to evaluate the kinetics of the macroscopic responses in the context of how rapidly agonist is washed in and out of the chamber. Based on these observations, it seems that the decay of the T6′F mutant responses follows the solution exchange rates much more closely than wild-type α7, suggesting that agonist washout may predominate in this phase of the response.

The α7 T6′F Mutation Increases ACh Potency Compared with Wild-Type α7. Concentration-response functions for wild-type α7 and TM2 T6′F mutant are shown in Fig. 4. A dramatic increase (> 10 fold) in ACh potency was seen for the net charge analysis of the T6′F mutant (Fig. 4, Table 2), compared with wild-type α7. Note that both net charge (area under the curve) and peak concentration response curves are shown to illustrate the differences in apparent ACh potency as a function of the analysis method used. Comparison of these analyses shows that, as reported previously (Papke and Papke, 2002), the net charge concentration response curve analysis of wild-type α7 receptor showed a large difference in apparent potency compared with peak current analysis. In contrast, the T6′F mutant showed less difference between the two methods, because of a loss of the

characteristic concentration-dependent fast desensitization of α7.

The α7 T6′F Mutation Abolishes Barium Permeability and Reduces Inward Current Rectification. Barium is frequently used as a charge carrier to evaluate divalent ion permeability because the relative permeability of barium to monovalent cations is generally indicative of calcium permeability, and the use of barium decreases the secondary signal transduction frequently associated with calcium influx. Current-voltage relationships obtained in either high or low extracellular barium, showed the characteristic wild-type α7 receptor inward rectification and permeability to this divalent ion (Fig. 5A) (Decker and Dani, 1990; Sands et al., 1993; Seguela et al., 1993; Vernino et al., 1994). The extended GHK equation gave an estimated barium-to-sodium permeability ratio of approximately 4:1. This ratio is substantially lower than that reported previously (Sands et al., 1993); however, this apparent discrepancy might be a result of the use of

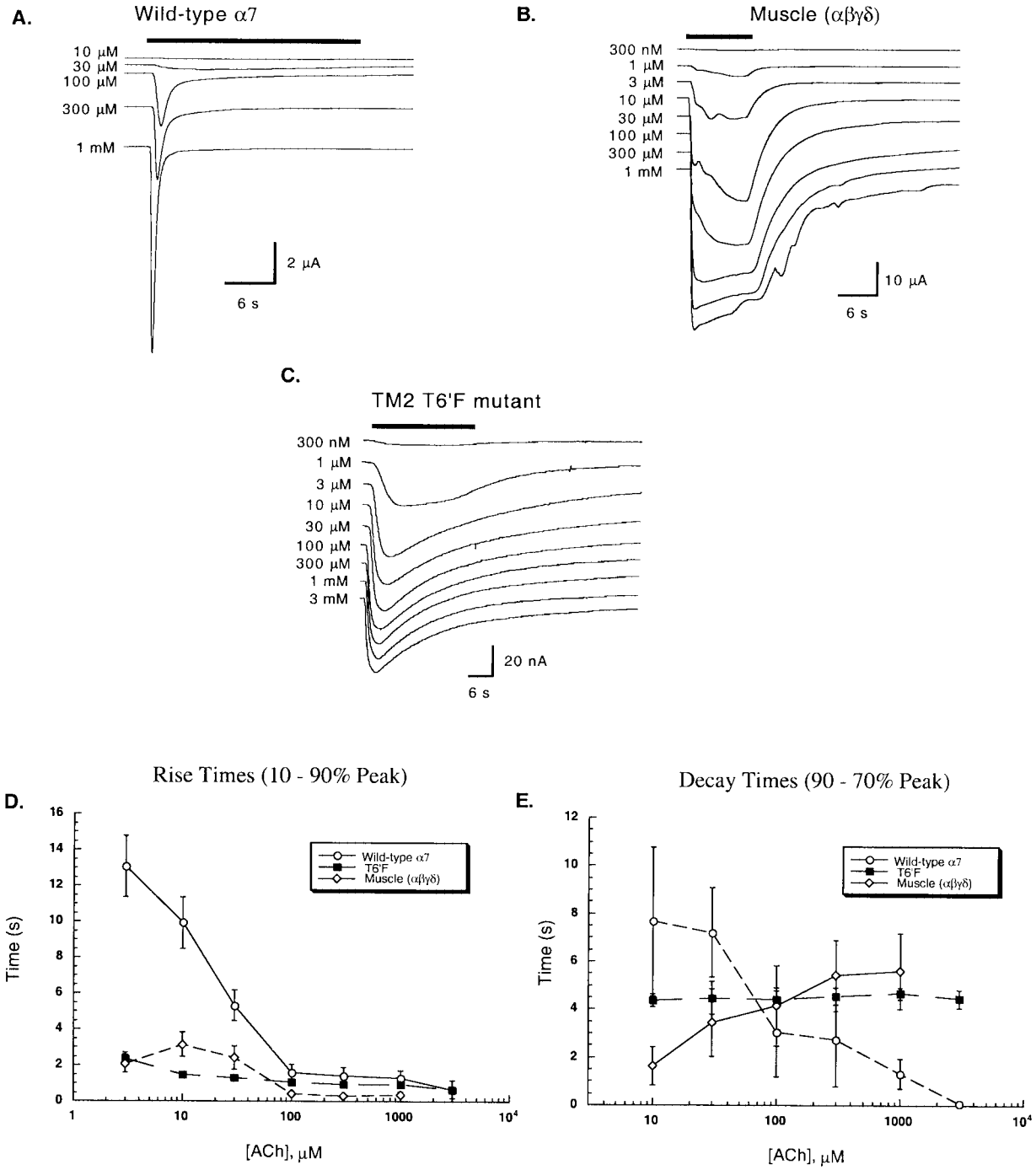

Fig. 3. Macroscopic response kinetics of wild-type α7, muscle, and the TM2 T6′F mutant nAChRs expressed in oocytes. A, wild-type rat α7 current traces at the indicated concentration of ACh. B, wild-type muscle (αβγδ) current traces at the indicated concentration of ACh. C, rat α7 TM2 T6′F current traces at the indicated concentration of ACh. D and E, rise times (10–90%) and decay times (90–70%) for macroscopic responses to ACh applied to each of the indicated receptors at the concentrations shown. The kinetics of muscle receptor responses as a function of increasing ACh concentration are also plotted for comparison. Means and S.E. are given for at least four cells.

EGTA in the current electrode solution. By contrast, the T6′F mutant receptor showed significantly less current rectification (Fig. 5B), as indicated by chord conductances measured between −40 and +30 mV holding potentials ($p = 0.003$ compared with wild-type α7, unpaired t test), and a complete lack of a shift in reversal potential with varying extracellular barium concentrations (Fig. 5B). The GHK equation applied to these results gives a barium-to-sodium permeability ratio near zero.

Succinylcholine Is a Selective Agonist of Muscle-Type Receptors and Is Also an Agonist of α7 T6′F Mutant Receptors. As shown in Fig. 6A, succinylcholine is an effective activator of muscle-type receptors, but it is relatively ineffective in activating wild-type α7. We see a dramatic increase in the sensitivity of the mutant α7 receptor to succinylcholine compared with wild-type. Figure 6B shows the concentration-response relationships for both ACh and succinylcholine applied to wild-type murine muscle receptors ($\alpha\beta\gamma\delta$). Although succinylcholine is a partial agonist of muscle-type receptors, it produces no activation of the heteromeric neuronal nAChR, $\alpha 3\beta 4$, at concentrations up to 1 mM (data not shown). The effect of the T6′F mutation (Fig. 6C) can be seen to dramatically increase both the potency and the maximum response to succinylcholine relative to wild-type α7, which responds only to concentrations of succinylcholine that exceed 1 mM. Whereas succinylcholine is a weak partial agonist of wild-type α7 receptors, it seems to be a full agonist of the T6′F mutant receptors.

The TM2 T6′F Mutation Abolishes Potentiation by 5-Hydroxyindole. Responses of α7 nAChRs to ACh can be enhanced by 5-hydroxyindole in oocytes expressing α7 (Gurley et al., 2000; Zwart et al., 2002). This effect is demonstrated in Fig. 7 in oocytes expressing wild-type α7, exposed to a coapplication of 300 μM ACh and 1 mM 5HI. As reported previously (Grantham et al., 2002), the 5HI effect did not impact the macroscopic kinetics of the inward current (Fig. 7A). In whole-cell voltage-clamp experiments, 1 mM 5HI also potentiates wild-type α7 expressed in transfected GH4C1 cells by 540 ± 75% (mean ± S.E.M., $n = 7$; data not shown). In contrast, oocytes expressing T6′F mutant receptors show a

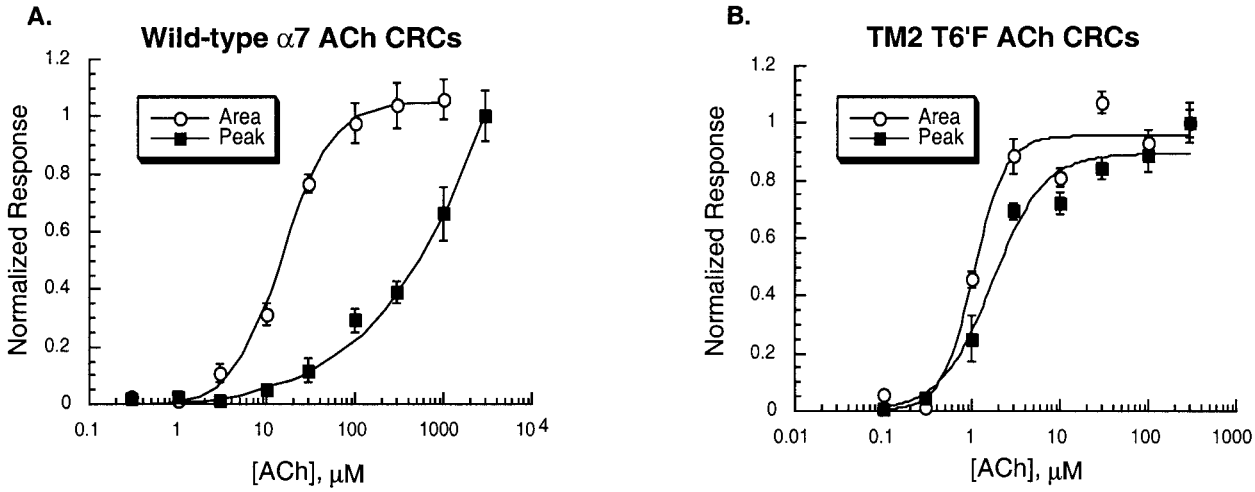

Fig. 4. ACh concentration-response functions for wild-type and the TM2 T6′F mutant α7 nAChR. Data were normalized to the maximal response for either wild-type rat α7 (A) or α7 TM2 T6′F (B). Peak and net charge analysis (area under the curve) are presented showing the relative sensitivity to increasing concentrations of ACh. Means and S.E. represent data acquired from at least four cells.

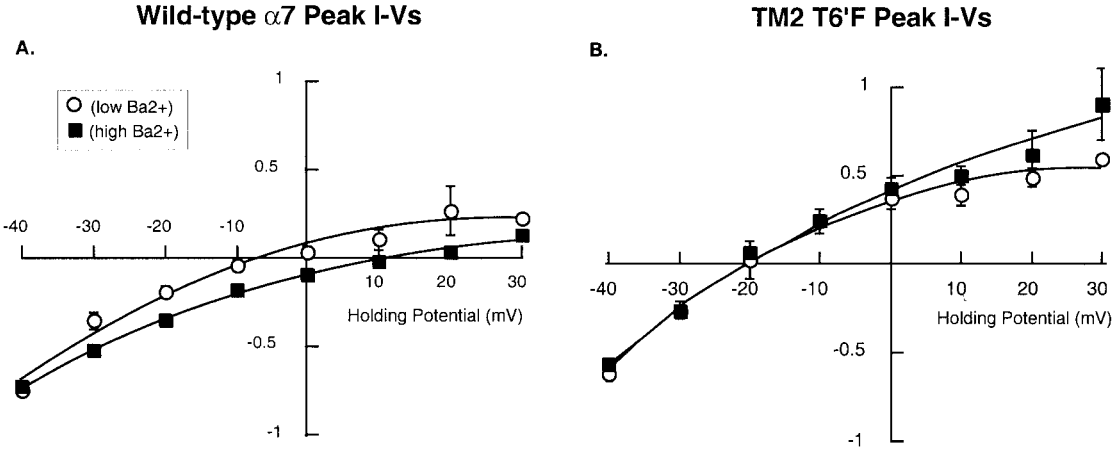

Fig. 5. Wild-type and mutant α7 nAChR current-voltage relationships and divalent ion permeability in *X. laevis* oocytes. Current-voltage relations were examined in wild-type α7 and T6′F mutant receptors using either high (18 mM) extracellular barium or low (1.8 mM) osmotically balanced extracellular barium. Holding potentials were incrementally adjusted by 10 mV from −40 to +30 mV and peak responses were normalized to control responses held at −50 mV. A, the wild-type α7 current-voltage relationship (I-V) shows its characteristic inward rectification, as well as positive shift in reversal potential with increased extracellular barium. B, the TM2 T6′F mutant current-voltage relationship shows less inward rectification, and the lack of a shift in reversal potential in high extracellular barium indicates a loss of divalent ion permeation.

total lack of enhancement of ACh evoked currents by 1 mM 5HI (Fig. 7, C and D). Comparing this lack of potentiation of T6′F mutant responses to the muscle-type nAChR shows an insensitivity identical to 5HI at the same concentration (Fig. 7, B and D).

Discussion

Although there are examples of single-point mutations producing dramatic changes in response kinetics, calcium permeability, and pharmacology of nicotinic receptors (Revah et al., 1991; Palma et al., 1996), the findings presented here are unusual in that several properties that functionally distinguish muscle-type nAChRs from members of the other major subgroups of nAChRs can be conferred to mutant α7 receptors by a single residue. This observation suggests not only the importance of amino acid sequence at this particular site for the maintenance of α7-like properties in the wild-type receptor but also that there is a high degree of functional significance to the structure at TM2 6′ position allowing a point mutation to overcome other distinguishing structural elements of the α7 subtype.

The relatively low magnitude of T6′F mutant receptor response to agonist compared with wild-type α7 is probably the result of a combination of factors. In the oocyte system, the loss of calcium permeability alone would diminish the functional amplification of the nAChR-mediated current by calcium-dependent chloride current (Barish, 1983). In addition, in the muscle receptors, the β subunit places a single phenylalanine at a site where it aligns with hydrophilic residues in the other subunits, whereas in the T6′F mutant α7 receptor, there is likely to be a complete hydrophobic ring at the same site in the channel. The positioning of a hydrophobic phenylalanine in the ion permeation pathway could therefore have profound effects on single channel properties. Based on the results of our radioligand binding experiments, we can conclude that there are comparable numbers (in the case of the oocytes, at least) of wild-type and T6′F mutant receptors expressed at the cell surface and that other factors may contribute to the mutant's relatively low response magnitude.

The variety of effects that we observed caused by the mutation of the TM2 6′ amino acid was intriguing, given the fact that this site is in the putative pore-lining region. The T6′F mutation converts α7 from a receptor having a high barium permeability to a receptor that is relatively impermeant to barium. This observation is not surprising given the likelihood of steric or hydrophobic interference (or both) to divalent ion flux through the pore related to the ring of phenylalanine residues present at the TM2 6′ position of the mutant receptor. Furthermore, others have reported that amino acids in the TM2 domain of several different ligand-gated ion channels (including α7) are essential determinants of ionic selectivity (Galzi et al., 1992; Keramidas et al., 2000; Gunthorpe and Lummis, 2001). More surprising about the findings presented here are the effects that this mutation has had on receptor properties that may be linked to conforma-

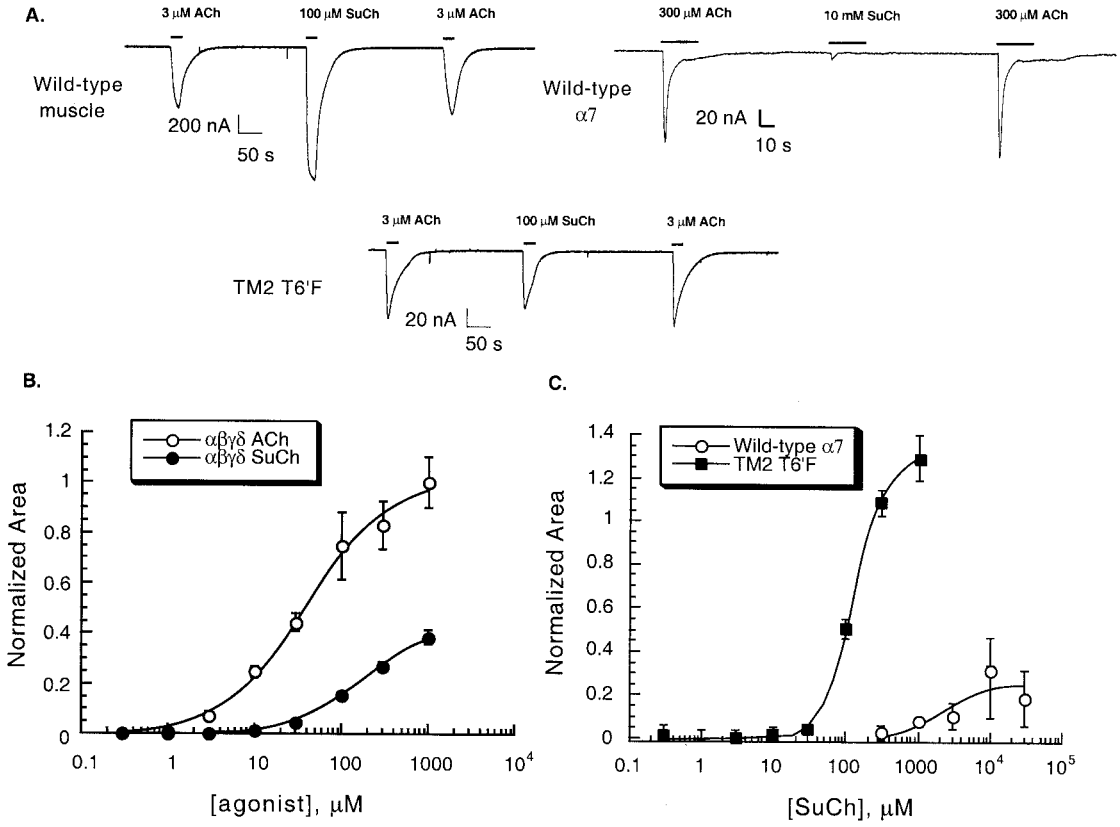

Fig. 6. Wild-type and mutant nAChR responses to the muscle receptor selective agonist succinylcholine. A, representative current traces for oocytes expressing the indicated nAChR subtype. The response to the indicated concentration of succinylcholine (SuCh) preceded and followed by control applications of ACh. B, net charge concentration-response relationships for wild-type muscle ($\alpha\beta\gamma\delta$) exposed to either ACh or SuCh. C, net charge concentration-response relationships for wild-type and the T6′F mutant α7 exposed to SuCh (see text for discussion of the use of net charge analysis for these experiments).

tional changes far removed from the pore-lining region (i.e., changes in succinylcholine pharmacology). It is thus likely that the T6′F mutation is indirectly impacting agonist binding, or that it is affecting the coupling of agonist binding and subsequent conformational effects, such as channel gating.

It is important to consider the findings presented here in the context of previous reports that indicate other contributing factors shown to regulate divalent ion permeability in muscle-type receptors. For instance, the muscle γ subunit has been shown to be an essential determinant of divalent cation permeability (Francis and Papke, 1996); however, one limitation of the experimental approach used in that study was the inability to evaluate the significance of the muscle β1 subunit. Thus, the γ subunit is necessary, but may not be sufficient, to produce the divalent ion permeability profile characteristic of muscle nAChRs. The results presented here imply that the β1 subunit, particularly the TM2 6′ phenylalanine, may cooperate with the γ subunit in determining this feature. It may be significant however, that the α7 TM2 T6′F mutant has five phenylalanine residues at this position compared with the muscle receptor's one, thus potentially amplifying the effect that this amino acid sequence has on wild-type receptor function.

The slowing of the macroscopic kinetics of the 6′ mutant receptor responses to ACh is reminiscent of the muscle-type receptors, with the decay phase of mutant receptor response kinetics showing a relative lack of sensitivity to changes in agonist concentration. This property is more characteristic of β subunit-containing receptors than wild-type α7 (Papke and Thinschmidt, 1998). The T6′F mutant response kinetics also show a nearly total lack of effect of ACh concentration on the rise rates of the macroscopic response. Again, this result seems to reflect the conferring of a non-α7 receptor-like property on the mutant. It is interesting to note that although the widely studied L9′T (L247T) mutation removes a great deal of the fast desensitization associated with the wild-type receptor (Revah et al., 1991), the amino acid substitution in nature is nearly opposite the one reported here. Although the

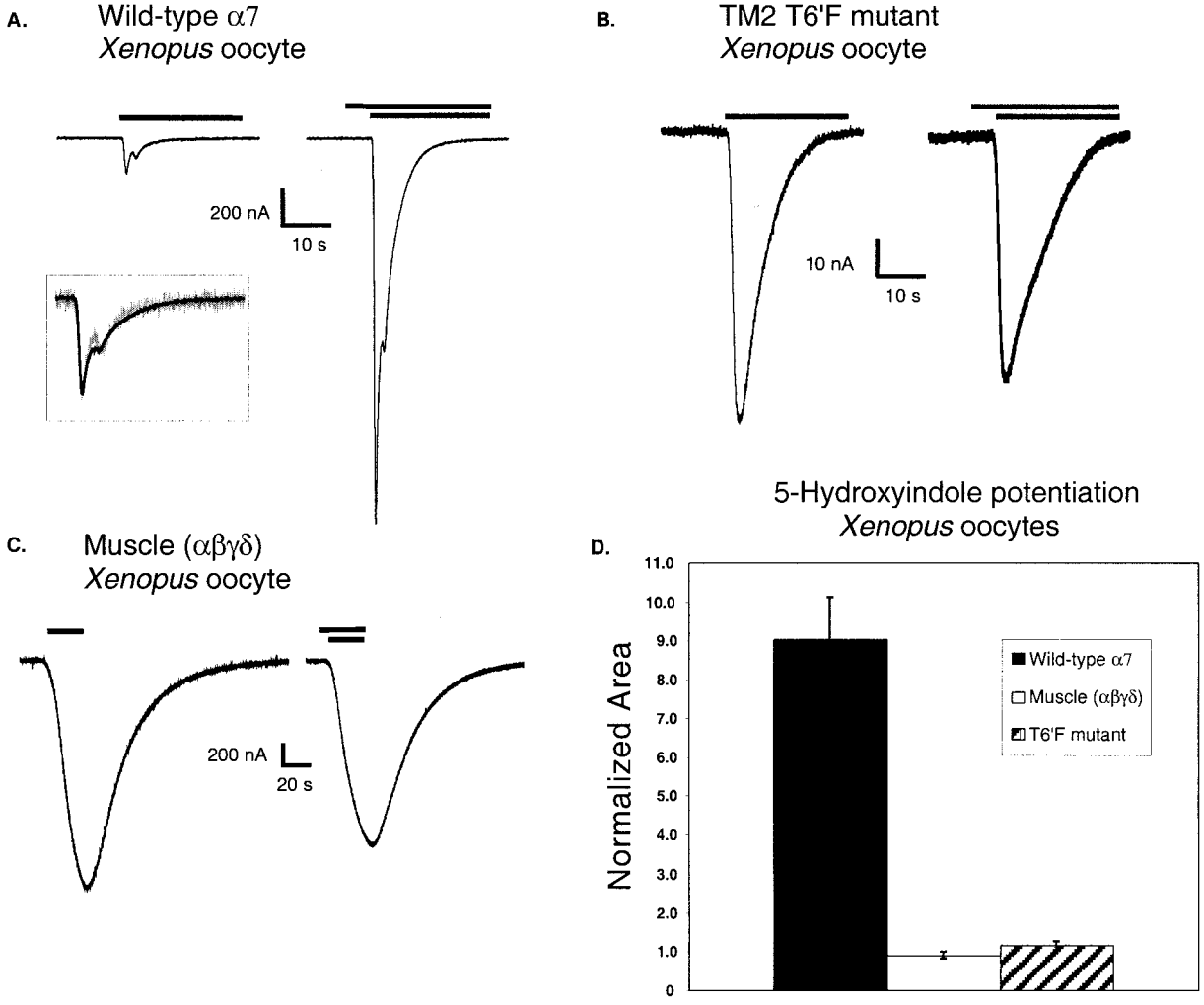

Fig. 7. Wild-type and mutant nAChR potentiation by 5-hydroxyindole. A, representative two-electrode voltage-clamp current traces from *X. laevis* oocytes expressing wild-type α7. Agonist application bars represent a control application of 300 μM ACh in the first trace and preincubation with 1 mM 5HI followed by coapplied 300 μM ACh. The inset shows the same two traces scaled to one another, showing the lack of an effect of 5HI potentiation on macroscopic response kinetics. B, representative current traces from *X. laevis* oocytes expressing the TM2 T6′F mutant receptor. The experimental design was similar to that described for the wild-type receptor above, except for the use of 3 μM ACh alone or coapplied with 1 mM 5HI. C, current responses representing a similar experimental design to that described above for oocytes expressing muscle-type nAChRs using 30 μM ACh alone or coapplied with 1 mM 5HI. D, the effect of coapplication of 1 mM 5HI on ACh responses normalized to the previous control application of ACh in *X. laevis* oocytes expressing the indicated wild-type or mutant nAChR subtype. Means and S.E. represent data from at least four cells.

L9′T represents the replacement of a larger, hydrophobic residue with a smaller hydrophilic one, the reverse is true for the T6′F mutation. This suggests that this aspect of the α7-type response may not be strictly regulated by size or hydrophobicity. Note that the 9′ leucine residue has been proposed to contribute to a ring of hydrophobic residues, whereas the 6′ threonine is more likely to contribute to a ring of polar residues approximately one level lower on the putative transmembrane helix, closer to the hypothetical selectivity filter of the channel (Corringer et al., 2000). In this regard, it is conceivable that substituted amino acids with different properties could be accomplishing a similar effect either through different mechanisms or through similar mechanisms at different sites in the receptor.

The conversion of succinylcholine from a very weak partial agonist of wild-type α7 receptors to a relatively potent full agonist of the T6′F mutant was an indication of the pharmacological constraints that these residues seem to place on their corresponding wild-type receptors. The fact that a significant degree of succinylcholine selectivity can be attributed to a residue in the pore lining region is perhaps less obvious, and is suggestive of more global effects of this amino acid on the overall structure of the receptor in both the open and closed states.

Although the mechanism of potentiation of α7 responses by 5-hydroxyindole is unknown, previous reports (Gurley et al., 2000) combined with our results from experiments with the muscle-type nAChR suggest that this effect may be unique to α7. The total absence of potentiation by 5HI for both the muscle and the T6′F mutant, compared with the expected large enhancement of ACh-evoked responses from wild-type α7, seems to be further confirmation of the ability of this amino acid substitution to imbue the mutant receptor with a muscle receptor phenotype. Without a clearer understanding of how 5HI potentiates wild-type α7 responses, it is difficult to suggest an explanation for its absence in the T6′F mutant. It is possible that amino acid sequence at the TM2 6′ position is an essential factor in the coupling of agonist evoked channel opening to an allosteric alteration produced by 5HI. On the other hand, the T6′F mutation may prevent 5HI from relieving a constitutive inhibition of wild-type α7, a mechanism that has been proposed for a similar potentiation of α7 by bovine serum albumin (Butt et al., 2002).

The data presented here suggest that the functional changes associated with the emergence of a specialized receptor involved in muscular contraction can be attributed, at least in part, to sequence difference at a single site in what is ultimately a structural subunit of the muscle receptor complex. It is potentially significant that the muscle β subunit is the only known nAChR gene product that contains a phenylalanine residue at this site (Le Novere and Changeux, 2001). The effects of this mutation extend beyond those that are commonly associated with amino acid structure in the pore-lining region of the receptor, and indicate that nAChR function and pharmacology can be broadly and dramatically altered by this single amino acid change. This suggests that the evolution of functional specialization in this superfamily of ligand-gated ion channels may involve something analogous to punctate equilibrium, where single small changes may produce branch points of functional significance and point to the origins of the families of receptor subtypes.

Acknowledgments

We thank Julia Porter Papke, Irena Garic, Bernadette Schoneburg, and Clare Stokes for technical assistance. We are very grateful to Axon Instruments for the use of an OpusXpress 6000A and pClamp9. We particularly thank Dr. Cathy Smith-Maxwell for her support and help with OpusXpress.

References

Barish ME (1983) A transient calcium-dependent chloride current in the immature *Xenopus* oocyte. *J Physiol* **342:**309–325.

Butt CM, Hutton SR, Marks MJ, and Collins AC (2002) Bovine serum albumin enhances nicotinic acetylcholine receptor function in mouse thalamic synaptosomes. *J Neurochem* **83:**48–56.

Chang Y and Weiss DS (1999) Channel opening locks agonist onto the GABAC receptor. *Nat Neurosci* **2:**219–225.

Corringer PJ, Le Novere N, and Changeux JP (2000) Nicotinic receptors at the amino acid level. *Annu Rev Pharmacol Toxicol* **40:**431–458.

Dani JA (2001) Overview of nicotinic receptors and their roles in the central nervous system. *Biol Psychiatry* **49:**166–174.

Davies AR, Hardick DJ, Blagbrough IS, Potter BV, Wolstenholme AJ, and Wonnacott S (1999) Characterisation of the binding of [3H]methyllycaconitine: a new radioligand for labelling alpha 7-type neuronal nicotinic acetylcholine receptors. *Neuropharmacology* **38:**679–690.

Decker ER and Dani JA (1990) Calcium permeability of the nicotinic acetylcholine receptor: the single-channel calcium permeability is significant. *J Neurosci* **10:** 3413–3420.

Fenster CP, Whitworth TL, Sheffield EB, Quick MW, and Lester RA (1999) Upregulation of surface alpha4beta2 nicotinic receptors is initiated by receptor desensitization after chronic exposure to nicotine. *J Neurosci* **19:**4804–4814.

Francis MM and Papke RL (1996) Muscle-type nicotinic acetylcholine receptor delta subunit determines sensitivity to noncompetitive inhibitors while gamma subunit regulates divalent permeability. *Neuropharm* **35:**1547–1556.

Galzi J-L, Devillers-Thiery A, Hussy N, Bertrand S, Changeux J-P, and Bertrand D (1992) Mutations in the channel domain of a neuronal nicotinic receptor convert ion selectivity from cationic to anionic. *Nature (Lond)* **359:**500–505.

Grantham CJ, Vandenberk I, and Ashton D (2002) Differentiation between the mechanisms by which ivermectin and 5-hydroxyindole positively modulate alpha7 nicotinic receptors. *Soc Neurosci Abstr* 137.3.

Gunthorpe MJ and Lummis SC (2001) Conversion of the ion selectivity of the 5-HT(3a) receptor from cationic to anionic reveals a conserved feature of the ligand-gated ion channel superfamily. *J Biol Chem* **276:**10977–10983.

Gurley D, Harris EW, Li C, Johnson EC, and Lanthorn T (2000) 5-Hydroxyindole potentiates the nicotinic acetylcholine receptor alpha7 subtype. *Soc Neurosci Abstr* **26:**827.

Keramidas A, Moorhouse AJ, French CR, Schofield PR, and Barry PH (2000) M2 pore mutations convert the glycine receptor channel from being anion- to cation-selective. *Biophys J* **79:**247–259.

Le Novere N and Changeux JP (2001) LGICdb: the ligand-gated ion channel database. *Nucleic Acids Res* **29:**294–295.

McGehee DS and Role LW (1995) Physiological diversity of nicotinic acetylcholine receptors expressed by vertebrate neurons. *Annu Rev Physiol* **57:**521–546.

Miller C (1989) Genetic manipulation of ion channels: a new approach to structure and mechanism. *Neuron* **2:**1195–1205**.**

Palma E, Mileo AM, Eusebi F, and Miledi R (1996) Threonine-for-leucine mutation within domain M2 of the neuronal alpha$_7$ nicotinic receptor converts 5-hydroxytryptamine from antagonist to agonist. *Proc Natl Acad Sci USA* **93:**11231–11235.

Papke RL and Papke JKP (2002) Comparative pharmacology of rat and human alpha7 nAChR conducted with net charge analysis. *Br J Pharmacol* **137:**49–61.

Papke RL and Thinschmidt JS (1998) The correction of alpha7 nicotinic acetylcholine receptor concentration-response relationships in *Xenopus* oocytes. *Neurosci Lett* **256:**163–166.

Revah F, Bertrand D, Galzi J-L, Devillers-Thiery A, Mulle C, Hussy N, Bertrand S, Ballivet M, and Changeux J-P (1991) Mutations in the channel domain alter desensitization of a neuronal nicotinic receptor. *Nature (Lond)* **353:**846–849.

Sands SB, Costa ACS, and Patrick JW (1993) Barium permeability of neuronal nicotinic acetylcholine receptor alpha 7 expressed in *Xenopus* oocytes. *Biophys J* **65:**2614–2621.

Seguela P, Wadiche J, Dinely-Miller K, Dani JA, and Patrick JW (1993) Molecular cloning, functional properties and distribution of rat brain alpha 7: a nicotinic cation channel highly permeable to calcium. *J Neurosci* **13:**596–604.

Vernino S, Rogers M, Radcliffe KA, and Dani JA (1994) Quantitative measurement of calcium flux through muscle and neuronal nicotinic acetylcholine receptors. *J Neurosci* **14:**5514–5524.

Webster JC, Francis MM, Porter JK, Robinson G, Stokes C, Horenstein B, and Papke RL (1999) Antagonist activities of mecamylamine and nicotine show reciprocal dependence on beta subunit sequence in the second transmembrane domain. *Br J Pharmacol* **127:**1337–1348.

Zwart R, De Filippi G, Broad LM, McPhie GI, Pearson KH, Baldwinson T, and Sher E (2002) 5-Hydroxyindole potentiates human alpha 7 nicotinic receptor-mediated responses and enhances acetylcholine-induced glutamate release in cerebellar slices. *Neuropharmacology* **43:**374–384.

Address correspondence to: Roger L. Papke, Department of Pharmacology and Therapeutics, Box 100267, JHMHSC, University of Florida, Gainesville, FL 32610-0267. E-mail: rpapke@college.med.ufl.edu